This article has been accepted for publication in a future issue of this journal, but has not been fully edited. Content may change prior to final publication. Citation information: DOI 10.1109/JSEN.2016.2532389, IEEE Sensors Journal

On energy hole and coverage hole avoidance in underwater wireless sensor networks

Kamran Latif[1], Nadeem Javaid[1,*], Ashfaq Ahmad[1], Zahoor Ali Khan[2], Nabil Alrajeh[3], Majid Iqbal Khan[1]

[1]COMSATS Institute of Information Technology, Islamabad 44000, Pakistan
[2]Internetworking Program, FE, Dalhousie University, Halifax B3J 4R2, Canada
[3]B.M.T, C.A.M.S, King Saud University, Riyadh 11633, Saudi Arabia
*Corresponding author: nadeemjavaidqau@gmail.com, www.njavaid.com

***Abstract*—Due to limited battery capacity of sensor nodes, minimization of energy consumption is a potential research area in Underwater Wireless Sensor Networks (UWSNs). However, energy hole and coverage hole creation leads performance degradation of UWSNs in terms of network lifetime and throughput. In this work, we address the energy hole creation issue in depth based routing techniques, and devise a technique to overcome the deficiencies in existing techniques. Besides addressing the energy hole issue, proposition of coverage hole repair technique is also part of this research work. In areas of dense deployment, sensing ranges of nodes redundantly overlap. Our proposed technique takes benefit of redundant overlapping and repairs coverage hole during network operation. Simulation results show that our two techniques cohesively conserve nodes' energy which ultimately maximizes the network lifetime and throughput at the cost of increased delay.**

***Keywords:* Coverage Hole, Routing, Energy Efficiency, Underwater Wireless Sensor Networks, Energy Hole**

I. Introduction

Given the persistent and critical water resource challenges in [1], applications of information and communication technologies can achieve water sustainability. In this regard, UWSNs play an important role as these deploy underwater sensors (nodes) to monitor the parameters of interest. The sensed information is then sent to off-shore sink(s) where it is interpreted to take proper actions; underwater communication is carried via acoustic modems and communication above the surface of water is carried via radio modems. In addition, recent research has shown manifold interest in underwater environment due to expanded application horizon including: detection of underwater oilfield reservoirs, exploitation of undersea minerals, providence of tsunami warnings, monitorship of undersea deployed expensive equipments, mine reconnaissance, [2], etc.

Irrespective of the application, nodes are exposed to harsh underwater environment that pose many challenges subject to long term operation of nodes. In UWSNs, the radio signals undergo rapid attenuation and high absorption rate. More specifically, the radio signals propagate in seawater only in extra low frequency range (i.e., $30 - 300$ Hz). However, this range requires high transmit power and large antennae. For example, the reported transmission range of Berkeley Mica 2 Motes is 120 cm at 433 MHz [3]. Data transmission or/and reception is thus not feasible via these signals. As an alternative, acoustic signals are typically used in such environments due to relatively low absorption rate. However, the acoustic signals have featured low bandwidth and relatively high end-to-end delay as underwater sensor nodes are sparsely deployed. The acoustic channel is highly impaired due to multi path and fading. Thus, high bit error rates are experienced. Furthermore, the underwater sensors are prone to failures due to fouling and corrosion. All these characteristics make the UWSN routing task very difficult. In addition, the UWSNs have highly dynamic topology that requires regular and frequent information exchange between network entities (nodes) if proper network operations are desired. However, these frequent and regular updates lead to significant routing overhead. Energy constrained nature of the nodes further demand for network lifetime maximization. Thus, network lifetime maximization, reliability improvement, efficient data gathering, and end-to-end delay minimization are always among the desired objectives when routing protocols are designed for UWSNs [4]-[5].

In [6], authors identify three subsystems in an underwater sensor; (i) sensing subsystem, (ii) processing subsystem and (iii) wireless communication subsystem. The first subsystem is used to acquire data, the second subsystem is used to process data and the third subsystem is used for communicating data. According to [7], these sensors perform collaborative monitoring tasks that involve high degree inter-sensor communications which lead to their high energy consumption cost. Authors in [8] point out the highly dynamic network topology of UWSNs which requires frequent exchange of messages (high overhead) among the sensor nodes for proper network functioning. Being small in size, the underwater sensors operate on tiny batteries (limited energy resource) to perform collaborative tasks [9]. Since most of the UWSN applications require large number of deployed sensors in harsh and highly unpredictable underwater environment, either infeasibility or almost impossibility to replace or recharge the batteries of these sensors further demand for network lifetime prolongation [7], [8]. Thus, improvement of energy efficiency is a potential research area in UWSNs because limited energy source of nodes is one of the major constraints in the long term operation of UWSNs. Therefore, intelligent and efficient utilization of energy is needed not only to prolong network lifetime but also to avoid creation of energy holes and coverage holes. In this regard, among other techniques of energy conservation, energy efficient routing plays an important role in conserving nodes' energy. In most of the underwater routing techniques, data packets travel from bottom to top in multi hop fashion. Sink nodes normally float

1530-437X (c) 2015 IEEE. Personal use is permitted, but republication/redistribution requires IEEE permission. See http://www.ieee.org/publications_standards/publications/rights/index.html for more information.

This article has been accepted for publication in a future issue of this journal, but has not been fully edited. Content may change prior to final publication. Citation information: DOI 10.1109/JSEN.2016.2532389, IEEE Sensors Journal

on water surface. Therefore, nodes near sink are engaged in heavy relaying of data which leads to the creation of energy hole and coverage hole. Another consequence of energy hole is network partitioning which ultimately leads to collapse of the entire network [10].

Coverage hole is the phenomenon which arises due to energy hole or regular death of a node. The area where coverage hole is created becomes un-sensed. In random deployment of nodes, it is also caused by uneven distribution of nodes in the network field. Because random deployment of nodes causes few areas of network to be more populated while leaving other areas less populated such that less populated network areas are more prone to coverage holes. In literature, many UWSN coverage hole repair techniques exist [11]-[12]. However, to our knowledge only [13] contributes regarding coverage hole avoidance at the time of deployment. Moreover, coverage repair process during network operation is not yet investigated in UWSNs. In this research work, which is extended form of our previous work in [14], we propose a coverage hole repair technique for UWSNs. Initially, we analyse depth based routing which enables us to identify the spots where most of the energy is consumed. Then, we propose a technique to balance the energy consumption of nodes. Our proposed technique not only identifies redundant coverage areas but also fills the hole area by moving nodes from redundant coverage areas to the hole area. Subject to evaluation of our proposed work, we conduct simulations and results justify its effectiveness in terms of the selected performance metrics. Thus, towards energy efficiency in UWSNs, our contribution will benefice the research community.

Rest of the paper is organised as: section II deals with related work and motivation, section III contains brief description of our proposed work, section IV calculates the coverage area and section V discusses the simulation results, finally conclusion and future work are given in section VI.

II. Related Work and Motivation

In [15], authors propose Depth Based Routing (DBR) technique for UWSNs. In order to send the sensed data packet towards sink, DBR uses an upward greedy approach. Nodes in the bottom of ocean sense data and nodes in the ocean columns act as forwarders. Each forwarder node maintains a list of neighbouring forwarder nodes which are at relatively lower depth and lie within a the threshold range. After receiving the data packet, forwarder nodes calculate Holding time (H_t) and then broadcast data packet to the next forwarder node. This process continues until data packet reaches the sink. DBR achieves high throughput, however, at the cost of high energy consumption, especially, dense areas lead to surplus energy consumption.

In order to improve the deficiencies of DBR, A. Wahid $et\ al.$ introduce Energy Efficient Depth Based Routing (EEDBR) [16]. In this technique, authors introduce Residual Energy (RE) factor for calculation of H_t. Due to the introduction of this factor, nodes with higher RE gain the priority of forwarding data. This technique balances the overall energy consumption in the network up to some extent. However, EEDBR achieves this goal at the cost of frequent knowledge sharing among nodes. Because RE of the nodes is continuously changing during network operation and if it is not timely updated then nodes may choose infeasible forwarders.

In [5], Vector Based Forwarding (VBF) is proposed. In VBF, a predefined path is established from source to sink in upward direction. Nodes in this path are the only eligible ones to forward the data packet. This method controls flooding in the network. However, in sparse network conditions, VBF's performance degrades due to unavailability of nodes along the predefined path which leads to high packet drop rate. Moreover, nodes' energy consumption is not uniform that may lead to early death of nodes along the path which can create a coverage hole or path breakage until its re-establishment.

M. Ayaz $et\ al.$ propose Hop-by-hop Dynamic Addressing Based (H2-DAB) routing protocol [17] for UWSNs. In this protocol, sink assigns hop IDs to all nodes. Nodes near sink get smaller ID and nodes away from sink get larger IDs. This is also a kind of depth information, that is node near sink have low depth and nodes away from sink have high depth value. However, data packet is always forwarded from higher ID nodes to lower ID nodes. Energy hole problem may arise here as lower ID nodes are near sink. Therefore, these are burdened with relaying load and their energy depletes at a relatively faster rate.

In [11], authors provide a technique for coverage hole repair of nodes on the basis of fuzzy logic. In the network field, mobile nodes are introduced during deployment phase. Whenever a node dies, mobile nodes locate dead node and decide which mobile node has to move to fill the hole. Performance of this protocol is satisfactory in low death rate of nodes, however, its performance degrades as the death rate of nodes increases because it becomes difficult for the limited number of mobile nodes to cover all these holes. This protocol focuses on hole repair for two dimensional deployment of nodes only.

HORA: A Distributed Coverage Hole Repair Algorithm for WSNs [12] assumes built in mobility feature in all nodes. When network starts operation, all nodes record neighbour information regarding overlapping of sensing ranges. Whenever, a node dies, neighbouring nodes move to fill the hole. The distributed algorithm decides which node has the highest priority to move first. HORA ensures no new coverage hole creation as a node moves to fill the existing coverage hole. Moreover, this work presents a two dimensional mathematical model for sensing disk overlapping of nodes.

In this paper, we are motivated from EEDBR [16] and HORA [12], and focus at their improvement in the following aspects.

- In EEDBR, frequent execution of Knowledge Acquisition Phase (KAP) consumes surplus energy. However, updating knowledge of nodes, on the basis of which nodes select next forwarder, is necessary. Therefore, KAP has to be frequently executed. However, KAP execution frequency setting leads to a trade-off between energy consumption and information update. We aim to minimize the energy consumption cost while keeping the nodes updated.
- In EEDBR, nodes use static transmission power level as per maximum transmission power level. As a con-

1530-437X (c) 2015 IEEE. Personal use is permitted, but republication/redistribution requires IEEE permission. See http://www.ieee.org/publications_standards/publications/rights/index.html for more information.

This article has been accepted for publication in a future issue of this journal, but has not been fully edited. Content may change prior to final publication. Citation information: DOI 10.1109/JSEN.2016.2532389, IEEE Sensors Journal

sequence, nodes waste energy incase of near transmissions. Thus, we aim at adaptive power control.

- In random deployment of nodes, uniform distribution of node density in the network field can not be guaranteed. Some places of the network field have high node density and vice versa. In energy constrained networks, node death is a regular phenomenon due to which coverage holes are created. Therefore, taking benefit of high node density, we introduce a hole repair mechanism. In this regard, we are motivated from hole repair technique presented in [12], where, authors presented energy hole detection and repair technique. Initially, they find overlapping of sensing discs and then filled the coverage hole by minimizing overlapping of sensing discs. However, in reality sensing area of a sensor is three dimensional. We transform the terrestrial sensing disc problem (two dimensional) into underwater spherical volume problem (three dimensional) and then provide a solution to fill the coverage hole(s). Since radio waves are not practical in underwater environment, we have replaced these with acoustic waves. For location information, we use Received Signal Strength Indicator (RSSI) as location finder [14], and use MoteTrack location identification scheme [15].

We are also motivated to address the following challenges among the mentioned ones in Section I.

- *Network lifetime maximization or energy efficiency improvement:* To maximize the energy efficiency of the network, our techniques routing is based on residual energy information of the nodes. Nodes need frequent update of routing information which leads to significant routing overhead. In order to reduce routing overhead, we used pic a back technique. With the help of this technique routing information is dynamically updated.
- *Packet loss minimization and multi-path fading avoidance:* Due to broadcast nature, wireless transmission is received by multiple in range nodes. If these nodes transmit at the same time, the intended destination is subject to high packet loss. SHORT implements holding time to overcome this issue. Moreover, this technique also avoids fading due to multi paths.

Moreover, the mentioned challenges are considered in the channel modeling. The channel model has a direct impact on nodes residual energy (based on which dead/alive nodes are calculated) and throughput. The proposed SHORT takes into account dead/alive nodes for repairing coverage holes which are created due to energy holes.

III. SHORT: Spherical HOle Repair Technique

Let the nodes are randomly deployed in a three dimensional underwater network area. In order to restrict the movement of nodes due to ocean currents these are anchored with wires and a floating mechanism [18] as shown in fig. 1. Variable length of wire with each node represents depth of a node. The longer the length of wire is, the shorter the depth of the node will be and vice versa. Sensor nodes (nodes) are assumed to sense underwater environmental data and transmit the sensed data to the sink nodes (sinks). We assume that all nodes are capable of acting as forwarders. These nodes are equipped with multi-power acoustic modems [19]. Thus, the nodes adjust their transmit power levels according to the location of intended next hop node. Sinks float on the surface of water and communicate with nodes and off-shore monitoring station via acoustic and radio modems, respectively. We assume that packet received at sink is delivered to monitoring station. The network model under discussion is assumed to be homogeneous in terms of initial energy and communication capabilities of all nodes.

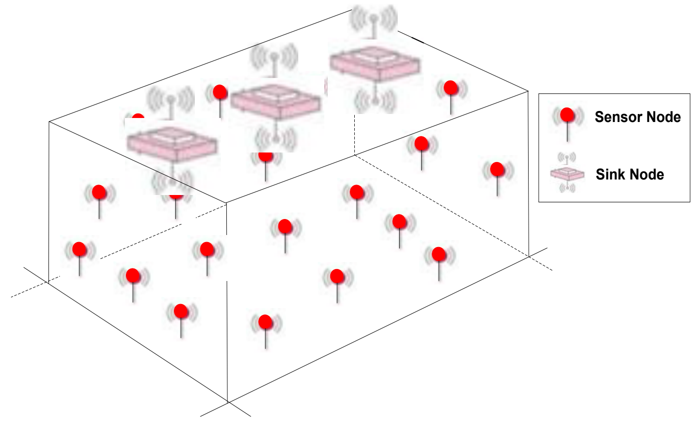

Fig. 1. UWSN: deployment of sensor nodes and sink nodes

Prior to the discussion of the proposed protocol operations, the underwater channel model needs to be discussed. Different factors affects sound propagation in sea [3]. As the sound travels from transmitter to receiver its intensity is reduced due to transmission loss. If S_i is the source intensity, SL is the source level and TL is the transmission loss then $S_i = SL - TL$. SONAR equation considers source level, sound spreading, absorption, reflection losses, ambient noise and receiver characteristics to calculate Signal to Noise Ratio (SNR). Therefore, $SNR = SL - TL - NL$. In the considered model, the losses due spreading, absorption and aggregate noise are calculated for acoustic channels. The total attenuation majorally depends on spreading and absorption losses. To calculate spreading loss, we use the model presented in [20]. Similarly, we use Thorp's model [21] to calculate absorption loss. According to Thorp's model, the absorption loss $a(.)$ for a given frequency f is calculated as follows:

$$10log\ a(f) = \begin{cases} \frac{0.11f^2}{1+f^2} + \frac{44f^2}{4100+f} + 286f^2 & \\ +0.003 & \text{if f} \geq 0.4 \\ 0.002 + 0.11\frac{f}{1+f} + 0.011f & \text{if f} < 0.4 \end{cases} \quad (1)$$

In (1), $a(.)$ is measured in dB/km and f is measured in kHz. If $A(l, f)$ denotes the total attenuation due to spreading and absorption then,

$$10log(l, f) = k \times 10log(l) + l \times 10log(a(f)) \quad (2)$$

where k denotes the spreading coefficient; $k = 1$ for cylindrical spreading, $k = 1.5$ for practical spreading, and $k = 2$ for spherical spreading [22]. In (III), the first term is spreading loss and the second term is absorption loss. To calculate the total ambient noise, four noise components

1530-437X (c) 2015 IEEE. Personal use is permitted, but republication/redistribution requires IEEE permission. See http://www.ieee.org/publications_standards/publications/rights/index.html for more information.

This article has been accepted for publication in a future issue of this journal, but has not been fully edited. Content may change prior to final publication. Citation information: DOI 10.1109/JSEN.2016.2532389, IEEE Sensors Journal

are considered; shipping noise $N_{shipping}$, thermal $N_{thermal}$, turbulence $N_{turbulence}$, and wind N_{wind}. We use the formula given in [3] to calculate the power spectral density of the four mentioned noise components as follows,

$$N(f) = N_{shipping}(f)+N_{thermal}(f)+N_{turbulence}(f)+N_{wind}(f) \quad (3)$$

where $10log(N_{shipping}(f)) = 40 + 20(s - 0.5) + 20log(f) - 60log(f + 0.03)$, $10log(N_{shipping}(f)) = 20log(f) - 15$, $10log(N_{turbulence}(f)) = 17 - 30log(f)$, and $10log(N_{wind}(f)) = 50+7.5w^{0.5}+20log(f)-40log(f+0.4)$.

We transform the terrestrial sensing disc problem (two dimensional) into underwater spherical volume problem (three dimensional) and then provided a solution to fill the coverage hole(s). By terrestrial sensing disc to underwater sensing sphere transformation, we not only mean geometric transformation but also channel transformation. This transformation is not just about replacing radio waves with acoustic waves, rather it takes into account the unique characteristics of underwater environment as discussed in the channel model.

Soon after node deployment, SHORT operation starts, which has the following three phases.

- Knowledge Sharing Phase (KSP)
- Network Operation Phase (NOP)
- Hole Repair Phase (HRP)

A. KSP

After deployment of nodes, KSP starts immediately. In this phase, each node shares depth, Residual Energy (RE) and location information through broadcast of hello packet. As common GPS does not work in underwater, buoy nodes based underwater GPS systems like PARADIGM [23] and GIB [24] have been proposed. Typically, the underwater GPS systems rely on buoy nodes at the surface of water to give absolute location; the buoy nodes act like satellites of common GPS. Nodes that lie with the communication range of buoy nodes are capable to estimate their distances to three nodes (at minimum). However, for large-scale UWSNs, the nodes are unable to get their absolute locations from the underwater GPS due to two reasons. Firstly, high cost hardware requirement hinders their deployment in practical underwater environments. Secondly, the surface buoy nodes must ensure that all the other nodes successfully receive their messages that requires large amount of transmit power. This requirement shortens the lifetime of buoy nodes as these are mostly powered by batteries. Besides the underwater GPS, authors in [23],[25] propose localization based protocols for underwater environment. However, these are not suitable for large-scale UWSNs due to direct communication requirement with the buoy nodes. In order to overcome the aforementioned deficiencies, we use Received Signal Strength Indicator (RSSI) as location finder [26], and use MoteTrack location identification scheme [27]. As for as mobility of nodes is concerned, we have only assumed vibrational motion because the nodes are anchored. Once identified, node's location can only be changed through HRP of SHORT.

Each node maintains two types of lists about its neighbouring nodes. The first list contains node IDs which are at lower depth from itself and within the D_{th} which is a system parameter and depends on transmission radius (R). Moreover, D_{th} is always less than R and increases as R increases. Nodes use information of this list for data forwarding. Node embeds IDs of this list in the data packet and then broadcast the data packet. Receiver nodes with matching IDs accept the data packet and all others discard it. During NOP, each node updates this list on receiving updated RE status through data packet. Dead nodes are discarded from this list time to time during the updates. The second list contains node IDs which are within sensing radius (r) of the node. This list is used to identify the status of the node as Cross Triangle (CT) node, Hidden Cross Triangle (HCT) node and Non Cross Triangle (NCT) node. Detailed discussion about how a node gain status of CT, HCT or NCT is given in section III-C.

In order to conserve network's energy, execution frequency of KSP is restricted. Initially, KSP is executed at network start-up, and it is then periodically executed prior to HRP. As SHORT data forwarding mechanism is based on node's RE and depth information, each node needs their regular updates. To fulfill this updating requirement, we use pick a back technique. In this technique, RE information is embedded within the data packet. In this way, the receiving nodes are updated within these information whenever a node broadcasts. Frequent execution of KSP means knowledge updation at a faster rate, however, at the cost of high energy consumption. Thus, there is a trade-off between execution frequency of KSP and energy consumption of nodes.

B. NOP

Completion of KSP triggers the start of NOP. In this phase, data packet is forwarded from source node to destination node that may or may not involve intermediate nodes. If the next hop node is sink, then the packet has reached its destination. If the next hop node is not sink, then the following three operations are performed.

- Data aggregation: As SHORT also handles column sensing applications all nodes except bottom nodes can perform forwarding task(s). The forwarding nodes transmits aggregated received data from other nodes and its own data to the next node.
- Holding time calculation: Each node transmits the received packet after waiting for the calculated H_t to expire. Where, each receiving node calculate its H_t with the help of following metric [16].

$$H_t = (1 - \frac{C_e}{I_e \times d}) \times Max_{H_t} + p, \quad (4)$$

where C_e is its current energy, I_e is its initial energy, Max_{H_t} is the maximum holding time which is a system parameter, d is depth of the node and p is the priority factor. The factor p uniquely identifies H_t among nodes and is the sequence numbers of forwarder nodes in which forwarder node IDs are stored. H_t is never same for two nodes of same depth and same RE. Nodes with lower depth and higher RE have smaller H_t.

- Data forwarding: On receiving data packet(s), the receiver node embeds IDs of all its neighbouring nodes

1530-437X (c) 2015 IEEE. Personal use is permitted, but republication/redistribution requires IEEE permission. See http://www.ieee.org/publications_standards/publications/rights/index.html for more information.

This article has been accepted for publication in a future issue of this journal, but has not been fully edited. Content may change prior to final publication. Citation information: DOI 10.1109/JSEN.2016.2532389, IEEE Sensors Journal

in the data packet, performs data aggregation and calculates holding time according to eqn. 4. After elapsing H_t or Max_{H_t}, the receiver node transmits the data packet. H_t mechanism is also used to suppress retransmission of same data packet. When a data packet with same ID is received by more than one nodes then after calculation of H_t, node with less H_t broadcasts the data packet and nodes with large H_t hears the data packet with same ID that these nodes already possess. In this way, these nodes suppress retransmission of same packet and thus conserve energy.

C. HRP

In order to maximize the lifetime of UWSN, it is necessary to maintain connectivity between nodes. As in depth based routing techniques, data packet travels from bottom to top, the death of a node in an established path of traffic flow not only creates hindrance in flow but also creates coverage hole (the area becomes un sensed). Our proposal determines that how this hole can be filled by moving neighbouring node(s).

When the energy level of a node reaches lower threshold, it announces its death status and stops working. All the neighbouring nodes become aware of the death announcement and start flooding this message throughout the network. In this way, HRP is activated. In KSP, each node records list of neighbours within *r*. Each node processes this list and declares itself as CT, HCT or NCT node. In the following sections, we present mathematical formulation of these processing steps.

1) Mathematical Formulation: Due to random deployment in UWSNs, nodes are densely deployed in few regions of the target area and sparsely in others. Nodes death is obvious during network operation due to many reasons. For example, due to energy hole or due to exhaustion of the battery. Irrespective of the reason, coverage hole is created. SHORT fills this hole by moving nodes from densely populated region(s). Let us consider a node N, r of N is represented as the spherical region S as shown in fig. 2. The relation between r and R is given by eqn. 5.

$$r = \frac{1}{2}R \tag{5}$$

Following are the definitions of few terms which are used in this research work [12].

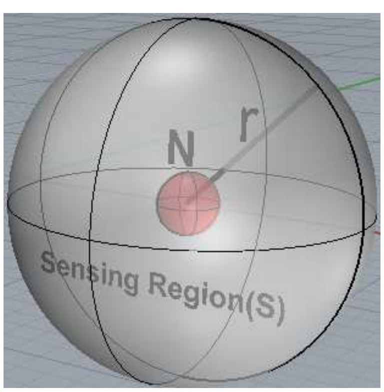

Fig. 2. Spherical region induced by sensing range of a sensor node

Surrounding Nodes: Let us consider few nodes with overlapped sensing ranges as shown in fig. 3. If N_i, $\forall i = 1, 2, 3, ..., m$ are one-hop neighbours of N_j, $\forall j = 1, 2, 3, ..., n$ and $i \neq j$ then the distance between j and i is given by; $0 < d_{j,i} < 2r$. If A_j is the surface area of S_j then SUM_{A_j} is the sum of surface areas induced by N_j and all its neighbours N_i, as shown in fig. 3(b) and is given by following equation.

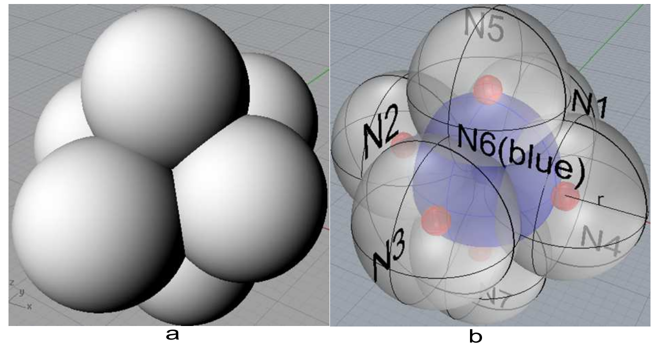

Fig. 3. Surrounding nodes

$$SUM_{A_j} = (A_j + \sum_{i=1}^{m} A_i) - (A_j \bigcap_{i=1}^{m} A_i) \tag{6}$$

$$such\ that \quad A_j \cap \sum_{i=1}^{m} A_i \neq A_j,$$

$$and \qquad A_j = 4\pi r^2$$

As shown in fig. 3(b) if *N6* dies, a coverage hole is created. All nodes intersecting coverage hole are known as surrounding nodes of this hole, therefore, *N1, N2, N3, N4, and N5* become surrounding nodes.

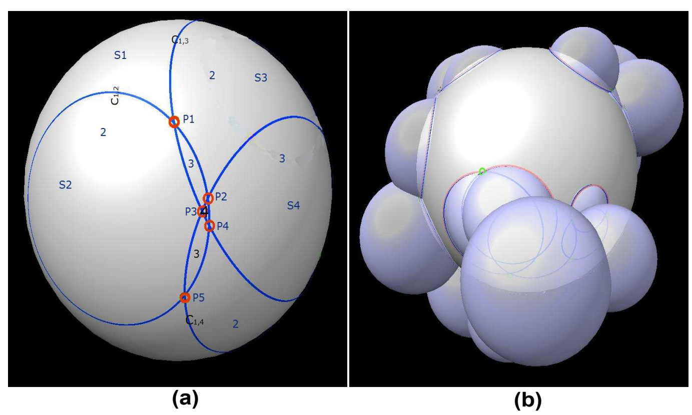

Fig. 4. (a) Illustration of O-cover and inclosing points (b) Spherical intersection

O-cover: In an intersection of two or more nodes, O-cover is the number of nodes that participate in the common overlapping area. However, if a node is overlaps with other nodes in different directions then it has more than one values of O-cover. For example in fig. 4, $S1$ intersects with $S2, S3$ and $S4$. Therefore, O-cover value of $S1$ with $S2$ is *2* and with $S2$ and $S3$ is *3*. Similarly, O-cover value of $S1$ with $S2$, $S3$ and $S4$ is *4*. Thus, O-cover(S1) contains the following list of values:

$$O - cover(S1) = [2, 2, 2, 3, 3, 3, 4] \tag{7}$$

1530-437X (c) 2015 IEEE. Personal use is permitted, but republication/redistribution requires IEEE permission. See http://www.ieee.org/publications_standards/publications/rights/index.html for more information.

This article has been accepted for publication in a future issue of this journal, but has not been fully edited. Content may change prior to final publication. Citation information: DOI 10.1109/JSEN.2016.2532389, IEEE Sensors Journal

m-max: Maximum value in the list of O-cover of a sphere. For example, m-max(S1) is given by eqn. 8.

$$m - max(S1) = 4 \tag{8}$$

Enclosing Points of a Node: Intersection of two spheres results in a circle as shown in fig. 4(b). Intersection of *S1 and S2* results in a circle $C_{1,2}$. Similarly, intersection of *S1, S3* and *S1, S4* results in circles $C_{1,3}$ and $C_{1,4}$, respectively as shown in fig. 4(a). The intersection points of these circles on the surface of *S* are known as enclosing points of *S*. Therefore, intersecting points *P1, P2, P3, P4, and P5* in fig. 4(a) are enclosing points of *S1*.

Cross Triangle (CT) Nodes: We consider the connectivity between nodes as a graph such that a node represents Vertex (V) of the graph and link between two nodes represents an Edge (E) of the graph. Order of the graph is the number of Vs in that graph. The graph, as a result of random deployment of nodes, represents a connected graph. However, few nodes of them are strongly connected; CT nodes represent strongly connected graph of order more than or equal to *4* and $m - max(CT) \geq 4$. Another property of CT nodes is that their connectivity in terms of graph represents two cross triangles as shown in fig. 5(a), nodes *N1, N2, N3*, and *N4* are therefore CT nodes.

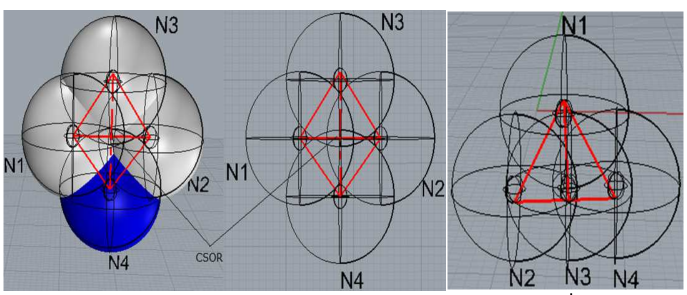

Fig. 5. CSOR of nodes: (a) CT nodes (b) HCT nodes

Hidden Cross Triangle (HCT) Nodes: HCT nodes also represent strongly connected graph of order more than or equal to *4*, however, at least three nodes of them must be linearly connected. Their connectivity represents two adjacent right triangles as shown in fig. 5(b), nodes *N2, N3, N4* are collinear therefore, *N1, N2, N3* and *N4* are HCT nodes.

Non Cross Triangle (NCT) Nodes: All nodes, except CT and HCT are NCT nodes.

Common Spherical Overlapping Region (CSOR): The common overlapping region of CT, HCT, or NCT nodes is defined as: CSOR $= \{g | g \in S_j \cap S_i$, where S_j and S_i ϵ *S, j* $\neq i\}$. Fig. 5(a) shows CSOR of nodes *N1, N2, N3*, and *N4*.

Mobile Node: The node which moves to fill the coverage hole is known as mobile node. A mobile node could be a CT, HCT, or NCT node, however, CT and HCT nodes have highest priority to become mobile node.

From the above definitions, we conclude that *CT* or *HCT* node is a strong candidate for mobility. Because these nodes cover redundant area and their movement do not create any new coverage hole. Therefore, now we establish a relation between number of *CT* or *HCT* nodes and their overlapping areas.

Corollary 1: m-max(CT—HCT) ≥ 4
Proof: Let us consider two connected nodes *N1* and *N2* such that $S1 \cap S2 \neq \phi$ and $0 < d_{1,2} < 2r$. As shown in fig. 5, nodes are co-linear however, not CT or HCT nodes because m-max($S1|S2$) ¡ 4. By method of induction, let us introduce another node *N3* between *N1* and *N2*, such that $0 < d_{1,2} < 2r$, $0 < d_{1,3} < 2r$, $0 < d_{2,3} < 2r$. From fig. 5, it is clear that nodes' connectivity forms a triangle, however, m-max(S1—S2—S3) ¡ 4. Therefore, by definition these are not CT or HCT nodes. Using method of induction again and introducing a new node *N4* between *N1*, *N2* and *N3* such that $0 < d_{1,2} < 2r$, $0 < d_{1,3} < 2r$, $0 < d_{1,4} < 2r$, $0 < d_{2,3}$, $0 < d_{2,4} < 2r$, and $0 < d_{3,4} < 2r$. This figure shows that *S1, S2, S3, S4* share same CSOR and their m-max = 4. Moreover, connectivity of all these nodes represents two cross triangles. Hence proved that m-max value of CT or HCT nodes must be ≥ 4.

2) Selection of Mobile Node: Before going to decide selection of mobile node, each node is considered as candidate node. Each candidate node observes the following two constraints prior to become a mobile node.

- A node which is going to be mobile must not lose its existing connectivity.

$$0 < d_{c_i,js} < 2r, \quad i \neq j \tag{9}$$

  where c_i is the candidate node and j_s are its adjacent nodes.
- Mobility of candidate node must not create any coverage hole.

All candidate nodes collect the following information about their one-hop surrounding nodes.
α**:** Cardinality of set of one-hop adjacent nodes with the following two conditions:
(a) Node(s) must not be part of the same CSOR with candidate mobile node.
(b) Node(s) must be a CT or HCT node.
If both a and b are true then $\alpha = x$, else $\alpha = 0$.

β**:** Cardinality of set of NCT nodes which are one-hop adjacent with candidate node with the following conditions:
If the candidate node is not a surrounding node then $\beta = x$, else $\beta = 0$.

γ**:** Number of NCT nodes of candidate node provided:
If the number of NCT nodes ≥ 1 then $\gamma = 1$, else $\gamma = 0$.

ρ : Number of intersection points within or on the surface of the spherical region induced by the candidate node. Value of ρ for N1 in fig. 4 is 5 because there are 5 intersection points on the spherical region induced by N1.

With the help of α, β, γ, and ρ, we can identify the neighbour distribution of a candidate node. After collecting these information each node calculates its own C_{val} by using the following formula:

$$C_{val} = \begin{cases} \beta - \alpha - \rho & : \beta > \gamma \ or \ \gamma = 0 \\ \gamma - \alpha - \rho & \end{cases}$$

1530-437X (c) 2015 IEEE. Personal use is permitted, but republication/redistribution requires IEEE permission. See http://www.ieee.org/publications_standards/publications/rights/index.html for more information.

This article has been accepted for publication in a future issue of this journal, but has not been fully edited. Content may change prior to final publication. Citation information: DOI 10.1109/JSEN.2016.2532389, IEEE Sensors Journal

Node(s) with highest C_{val} is(are) selected as mobile node(s), however, more than one candidate nodes further decide on the basis of shortest distance from the hole location.

3) Selection of Assistant Node: Each mobile node has to decide with which adjacent node it has to reduce overlapping. The node, which mobile node selects to reduce overlapping is known as assistant node. Selection of assistant node helps in finding the amount of distance to move for mobile node. As mobile node knows the locations of all its surrounding nodes, therefore, it calculates angle (θ) formed with each one-hop adjacent neighbouring node with the help of hole location. Mobile node selects node with maximum value of (θ) as its assistant node. For example in fig. 6, if N4 is the mobile node and N6 is the hole location. N4 measures value of θ with N1, N2, N3, and N5.

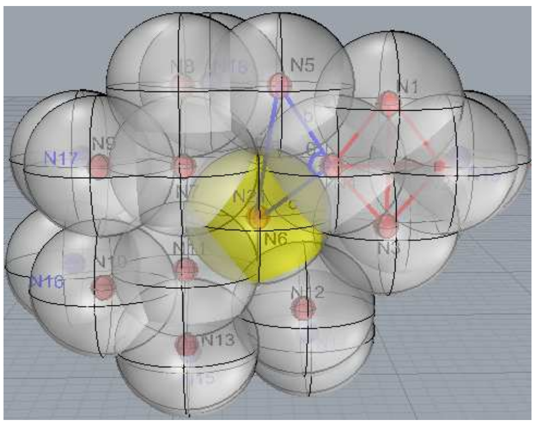

Fig. 6. Selection of assistant node

Consider $\triangle$ N5N6N4 to find the $\angle\Theta$. Sides of this triangle are a, b, and c. Using law of cosine the $\angle\Theta$ can be find out from the following equation.

$$\Theta = \arccos\left(\frac{b^2 + c^2 - a^2}{2bc}\right) \tag{10}$$

If there are i one-hop neighbours then $\angle$Assistant Node $=$ $max(\Theta_i)$. In this case N1 forms maximum angle with N4, therefore, N1 is selected as the assistant node of N4.

4) Distance and Direction of Mobile Node to Move: Mobile node could be CT, HCT, or NCT node. In this section, we discuss these individually.

Case 1: ***Mobile node is a CT or HCT node***

CT or HCT node calculates overlapping area with its assistant nodes. In order to avoid creation of new coverage hole due to mobility, mobile node can only move till the overlapping distance. Consider nodes N1, N4, and N6 in fig. 6. Where N6 is the hole location, N4 is the mobile node and N1 is the assistant node of N4. Let position coordinates of N4 are (0,0,0) and of node N1 are (d,0,0). We calculate the overlapping distance between N4 and N1 in the following way.

$$x^2 + y^2 + z^2 = r^2 \tag{11}$$

$$(x - d)^2 + y^2 + z^2 = r^2 \tag{12}$$

Solving eqns. 11 and 12 for x we get,

$$x = \frac{1}{2}d \tag{13}$$

Placing the value of x in eqn. 11 and solving we get,

$$y^2 + z^2 = \frac{1}{2}\sqrt{4r^2 - d^2} \tag{14}$$

Eqn. 14 is the equation of circle with radius (a) as shown in fig. 7.

$$a = \frac{1}{2}\sqrt{4r^2 - d^2} \tag{15}$$

Intersection of two spheres always result in a lens shaped

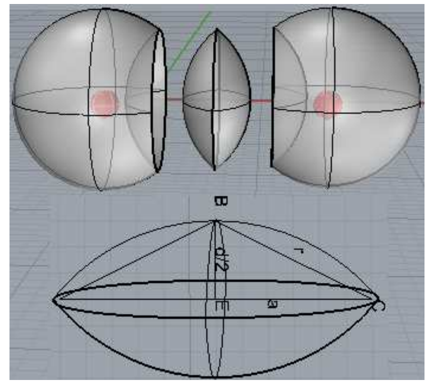

Fig. 7. Overlapping distance of sensing ranges of two nodes

region as shown in fig. 7. The hight (radius) of this lens is calculated in eqn. 15. Now we calculate the width of this lens. This problem is now similar to circle circle intersection. Consider the right triangle BEC, by using pythagorean theorem we can find (d) as follows.

$$\frac{d^2}{4} = \frac{a^2}{4} + r^2 \tag{16}$$

$$d = \frac{1}{2}\sqrt{4a^2 + r^2} \tag{17}$$

With the help of eqn. 17, we find how much a node can move. If the co-ordinates of mobile node are M(x1, y1, z1) and the co-ordinates of dead node are H(x2, y2, z2), then algorithm 1 finds the co-ordinates of new location for mobile node to move.

Case 2: ***Mobile node is a NCT node***

If more than one NCT nodes are surrounding nodes, then node with highest O-max value moves first. It finds its assistant node with the help of eqn. 10 and using algorithm 1 calculates its new location co-ordinates. After completion of its mobility, next NCT surrounding node with second highest value of O-max starts its movement in the similar way. This process continues until all surrounding NCT nodes complete their movement to fill the hole.

Case 3: ***Cascading mobility of CT/HCT and NCT nodes***

Prior to their movement, the NCT nodes broadcast an invitation message to CT/HCT nodes in their vicinity to move first, thus take the benefit of their overlapping. A CT/HCT node when hears an invitation message, it first checks its qualification for movement then the CT/HCT node moves as in CASE 1. NCT node then calculates its overlapping distance with neighbouring CT/HCT node according to eqn. 17 and finds co-ordinates of new location using algorithm 1.

If NCT node does not find any neighbouring CT/HCT node

1530-437X (c) 2015 IEEE. Personal use is permitted, but republication/redistribution requires IEEE permission. See http://www.ieee.org/publications_standards/publications/rights/index.html for more information.

This article has been accepted for publication in a future issue of this journal, but has not been fully edited. Content may change prior to final publication. Citation information: DOI 10.1109/JSEN.2016.2532389, IEEE Sensors Journal

Algorithm 1 Find coordinates of new location

INITIALIZATIONS
  dist-to-move = d
  SP(x_1, y_1, z_1) //Start Point Co-ordinates
  PP(x_p, y_p, z_p) = SP //Previous Point Co-ordinates
  HP(x_2, y_2, z_2) //Hole Point Co-ordinates
  LP(x_l, y_l, z_l) = HP //Last Point Co-ordinates
  PointFound = FALSE
  mid-point($x_m = \frac{(x_1+x_2)}{2}$, $y_m = \frac{(y_1+y_2)}{2}$, $z_m = \frac{(z_1+z_2)}{2}$)
  new-dist = $\sqrt{(x_2-x_1)^2+(y_2-y_1)^2+(z_2-z_1)^2}$
END INITIALIZATIONS
while(NOT PointFound)
if (new-dist == dist-to-move) **then**
  PointFound = TRUE
  RETURN mid-point
else
  if (new-dist > dist-to-move) **then**
    LP = mid-point
    mid-point($x_m = \frac{(x_m+x_p)}{2}$, $y_m = \frac{(y_m+y_p)}{2}$, $z_m = \frac{(z_m+z_p)}{2}$)
  else
    PP = mid-point
    mid-point($x_m = \frac{(x_m+x_l)}{2}$, $y_m = \frac{(y_m+y_l)}{2}$, $z_m = \frac{(z_m+z_l)}{2}$)
  end if
end if
new-dist = $\sqrt{(x_m-x_1)^2+(y_m-y_1)^2+(z_m-z_1)^2}$
end while

then first it finds its assistant node and then moves in the direction of hole using algorithm 1.

It is worth mentioning here that our proposed scheme will cause relatively higher delay as it involves relatively more calculations. However, we focus on the improvement of energy efficiency and throughput. Thus, we achieve our objectives at the cost of increased delay.

IV. Coverage Volume Calculation

Either a node moves to fill the detected energy hole or a node does not move to fill the energy hole (due to infeasible conditions). In both cases, the coverage volume is affected and needs to be calculated or re-calculated. It is worth mentioning here that spheres are drawn as circles in fig. 8 and fig. 9 only for the sake of simplicity in drawing.

Let V_i be the coverage volume of i^{th} node such that the total coverage volume of two overlapping spheres (refer fig. 8) is given by the following equation.

$$Cov_2 = V_1/V_2 + V_2/V_1 + M(V_1, V_2) \tag{18}$$

where, $M(V_1, V_2)$ denotes the mutual region between V_1 and V_2 (i.e., $M(V_1, V_2) = V_1 \bigcap V_2$), V_1/V_2 denotes part of V_1 that exclude V_2 (i.e., $V_1/V_2 = V_1 - M(V_1, V_2)$), and V_1/V_2 is part of V_1 that exclude V_2. Similarly, the coverage volume of three overlapping spheres (refer fig. 9) is calculated as follows.

$$Cov_3 = Cov_2 + V_3/(V_1, V_2) \tag{19}$$

where $V_3/(V_1, V_2)$ is part of V_3 that exclude V_1 and V_2, i.e., $V_3/(V_1, V_2) = V_3 - \{M(V_3, V_1) + M(V_3, V_2) - M(V_3, M(V_1, V_2))\}$. If a 4^{th} node is added to the network, then the total coverage volume is calculated by the following equation,

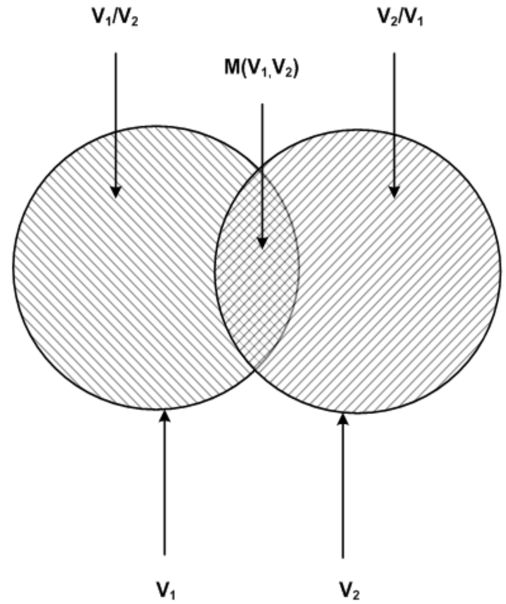

Fig. 8. Coverage overlapping due to two nodes

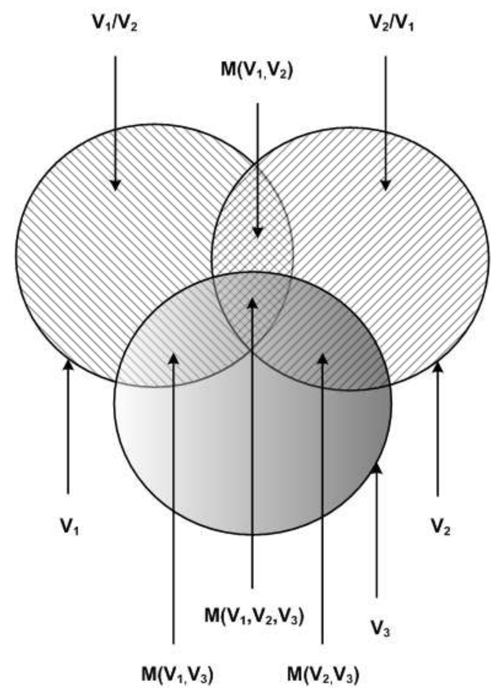

Fig. 9. Coverage overlapping due to three nodes

$$Cov_4 = Cov_3 + V_4/(V_1, V_2, V_3) \tag{20}$$

However, random node deployment further complicates the solution because the newly added node's coverage volume may overlap with one, more than one or none of the coverage volumes due to existing nodes. Thus, to account for this situation, we introduce connectivity parameter between node i

1530-437X (c) 2015 IEEE. Personal use is permitted, but republication/redistribution requires IEEE permission. See http://www.ieee.org/publications_standards/publications/rights/index.html for more information.

This article has been accepted for publication in a future issue of this journal, but has not been fully edited. Content may change prior to final publication. Citation information: DOI 10.1109/JSEN.2016.2532389, IEEE Sensors Journal

and node j as follows.

$$k_{(i,j)} = \begin{cases} 1, & \text{if } M(i,j) > 0 \\ 0, & \text{if } M(i,j) = 0 \end{cases}$$

This formulation leads us to a generalization that whenever a node is added to the network, only its non-overlapping coverage volume is added to the existing coverage volume. Therefore, the total coverage volume due to n randomly deployed nodes is calculated by the following generalized piece-wise equation.

$$Cov_i = \begin{cases} V_1, & \text{if } i = 1 \\ V_1/V_2 + V_2/V_1 + M(V_1, V_2), & \text{if } i = 2 \\ V_1/V_2 + V_2/V_1 + M(V_1, V_2) + \\ \sum_i V_i/(k_{(i,1)}V_1, ..., k_{(i,i-1)}V_{i-1}), & \text{if } i > 2 \end{cases}$$

V. Simulation Results and Discussions

In our simulation setup, nodes are randomly deployed in *100m* × *100m* × *100m* network volume. Subject to different scenarios, varying number of nodes (that ranges from *200* to *700*) are deployed. Transmission range of a node is assumed to be double of its sensing range. Five sinks are deployed with even space between them. Nodes are deployed with anchors and floating mechanism. Initially, all nodes are energised with homogenous resources. Nodes are equipped with acoustic modems. Depending upon the nature of application different acoustic modems can be used having different characteristics. However, all acoustic modems possesses characteristics of transmission range, transmission power levels, and lifetime of the battery. From application and energy consumption perspective it, is important to know that how much energy a modem consumes in transmit, receive and idle mode. Therefore, the model of the modem we used in our simulation consumes *2.5mW* power in standby mode, *5-285mW* power in in listening mode and *1.1mW* power in receive mode. For transmission it has three different ranges: *250m*, *500m* and *100m*. For these ranges it consumes power as *5.5W*, *8W*, and *18W*, respectively. As each node is capable of transmitting over multiple transmission ranges therefore, in simulation setup, we assumed transmission ranges as; *75m*, *50m* and *25m*. Parameters of the Physical and MAC layers are kept same as in [16]. Subject to throughput calculation, we use the packet drop model presented in [28]. In order to evaluate our proposed work, we use two metrics; alive nodes, and throughput. We run our simulations five times and average results are plotted.

In our technique, *CT* and *HCT* nodes have direct relation with node density. Fig. 10 shows that are deployed with varying densities of *200* to *700*. We have assumed *35m*, *45m* and *55m* sensing ranges. The result shows that as node density increases number of *CT/HCT* nodes increases. The combined effect of longer sensing range and higher node density produce large number of these nodes.

Similarly, results in fig. 11 show that dense deployment of nodes and long sensing range create relatively high overlapping. It implies that overlapping of nodes is directly proportional to to the formation of *CT/HCT* nodes. Our technique benefice the network by making these nodes as sleep nodes. When any of the sleep node becomes boundary node to repair the coverage hole, it is awaken.

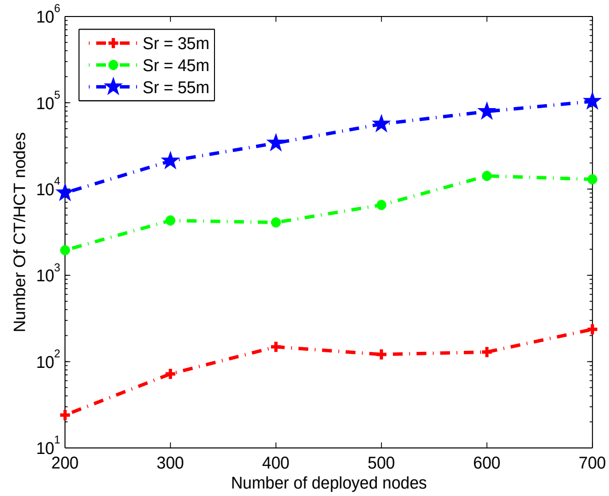

Fig. 10. Combined effect of sensing range and deployed nodes on CT/HCT nodes

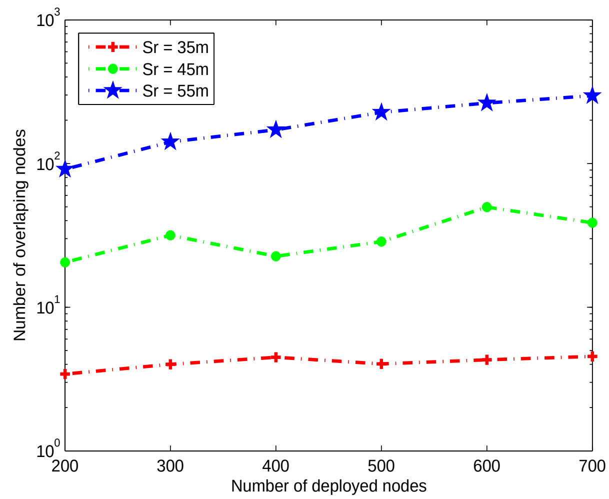

Fig. 11. Combined effect of sensing range and deployed nodes on overlapping nodes

Fig. 12 shows that coverage volume grows exponentially with increase in node density. As dense node deployment leads to relatively high overlapping volume which means that more volume is covered and the chances of coverage hole are thus minimized as for as initial phases of the network operations are considered.

From fig. 13, it is evident that network lifetime of SHORT is *59%* more than EEDBR and *145%* more than DBR. The possible reasons are: SHORT conserves energy via pick a back technique, SHORT saves energy by using multiple power transmission levels SHORT sleeps CT/HCT nodes which are redundant in the initial phase of the network operation. The initial nodes of SHORT die early, the reason is that initially due to few sleep nodes, less number of nodes participate in the network operation, therefore, forwarding load on few nodes increases. However, it does not affect the network lifetime as sleep nodes replace the dead nodes. In addition to the

1530-437X (c) 2015 IEEE. Personal use is permitted, but republication/redistribution requires IEEE permission. See http://www.ieee.org/publications_standards/publications/rights/index.html for more information.

This article has been accepted for publication in a future issue of this journal, but has not been fully edited. Content may change prior to final publication. Citation information: DOI 10.1109/JSEN.2016.2532389, IEEE Sensors Journal

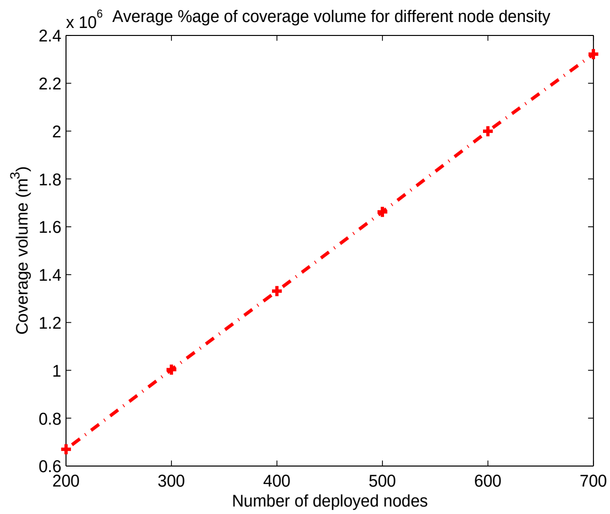

Fig. 12. Growth in coverage volume by increasing node density

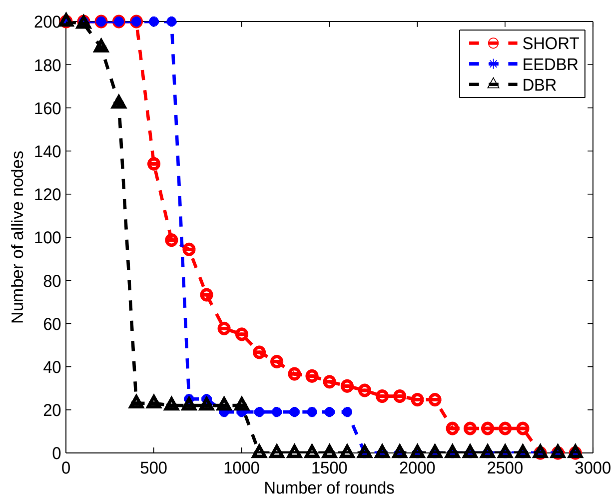

Fig. 13. Rate of alive nodes

above mentioned reasons, nodes in DBR and EEDBR actively participate in the network operations that lead to high energy consumption. Especially, in case of DBR, as it is not energy aware most of the nodes die during initial phase of the network operation.

Fig. 14 shows that throughput of SHORT is higher than its competitor protocols. Main reason behind higher throughput is nodes' longer lifetime. Sleep nodes take over the responsibility of forwarding data packet as any of the boundary node dies. Therefore, more nodes send data packets for longer period of network lifetime.

End to end delay of SHORT is higher than the competitor techniques as shown in Fig. 15. The basic reason behind higher end to end delay is processing time for removing coverage hole. As our hole repair algorithm is distributed therefore, all nodes involve in the coverage hole repair process which consumes time and ultimately affects packet delivery time. The cost of end to end delay is paid to achieve the benefits of

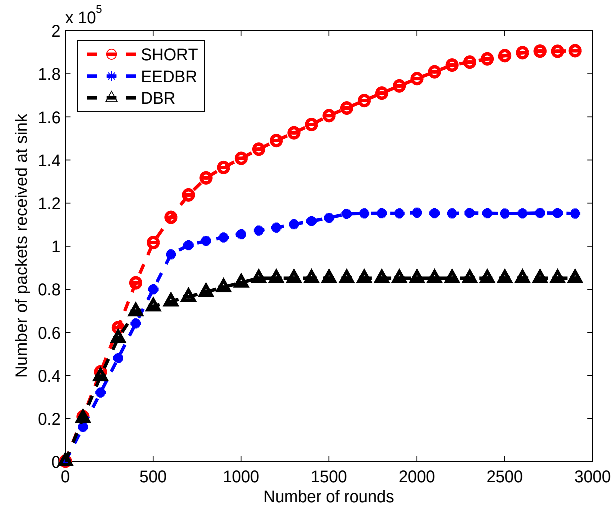

Fig. 14. Packets reception rate at sink

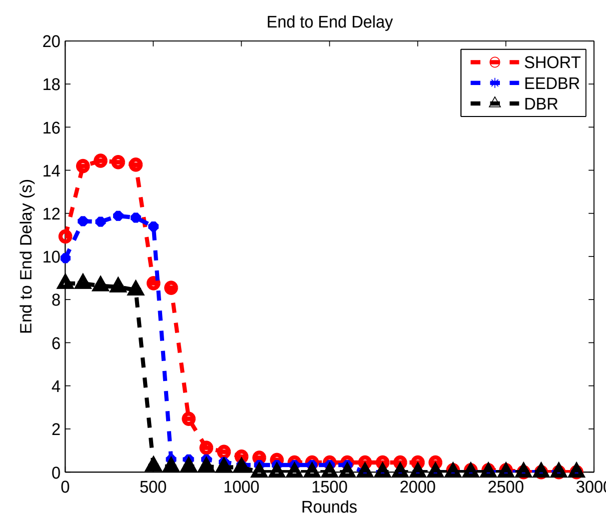

Fig. 15. End to end delay

network connectivity, throughput and energy conservation.

VI. Conclusion and Future Work

Energy hole and coverage hole are among the issues that degrade performance of UWSNs in terms of network lifetime and throughput. The former is created due to unbalanced or extra energy consumption of nodes in the network. The later one may arise due to energy hole, regular death of a node or random deployment of nodes. In our work, we addressed these issues in depth based routing techniques; DBR and EEDBR. We identified the processes in the protocol operation where most of the energy is consumed (for example, in KSP and static transmission power level). To solve these problems, we introduced a technique which reduces energy consumption in KSP and we also used different transmission power levels. These improvements significantly enhanced the network lifetime and throughput. We addressed the coverage hole issue by introducing hole repair technique. This technique first finds redundant coverage overlapping of nodes around the

1530-437X (c) 2015 IEEE. Personal use is permitted, but republication/redistribution requires IEEE permission. See http://www.ieee.org/publications_standards/publications/rights/index.html for more information.

This article has been accepted for publication in a future issue of this journal, but has not been fully edited. Content may change prior to final publication. Citation information: DOI 10.1109/JSEN.2016.2532389, IEEE Sensors Journal

coverage hole, and then repairs this hole by moving nodes covering redundant volume. However, movement of a node is restricted to overcome the creation of new coverage hole. Finally, we validated improved performance of our work in terms of the selected performance metrics through comparative simulations.

The energy hole detection and avoidance problem becomes more interesting if the nodes are not anchored. However, this requires a lot of extra work and we have future plans of doing so. Moreover, real time experimental test bed development for both static and mobile UWSNs is under consideration.

REFERENCES

[1] Z. Wang, H. Song, D. W. Watkins, K. G. Ong, P. Xue, Q. Yang, and X. Shi, "Cyber-physical systems for water sustainability: challenges and opportunities," *Communications Magazine, IEEE*, vol. 53, no. 5, pp. 216–222, 2015.

[2] I. F. Akyildiz, D. Pompili, and T. Melodia, "Underwater acoustic sensor networks: research challenges," *Ad Hoc Networks*, vol. 3, no. 3, pp. 257 – 279, 2005.

[3] I. F. Akyildiz, D. Pompili, and T. Melodia, "Underwater acoustic sensor networks: research challenges," *Ad hoc networks*, vol. 3, no. 3, pp. 257–279, 2005.

[4] H. Luo, Z. Guo, K. Wu, F. Hong, and Y. Feng, "Energy balanced strategies for maximizing the lifetime of sparsely deployed underwater acoustic sensor networks," *Sensors*, vol. 9, no. 9, pp. 6626–6651, 2009.

[5] P. Xie, J.-H. Cui, and L. Lao, "Vbf: vector-based forwarding protocol for underwater sensor networks," in *Networking 2006. Networking technologies, services, and protocols; performance of computer and communication networks; mobile and wireless communications systems*, pp. 1216–1221, Springer, 2006.

[6] F. K. Shaikh and S. Zeadally, "Energy harvesting in wireless sensor networks: A comprehensive review," *Renewable and Sustainable Energy Reviews*, vol. 55, pp. 1041–1054, 2016.

[7] I. S. Kulkarni and D. Pompili, "Task allocation for networked autonomous underwater vehicles in critical missions," *Selected Areas in Communications, IEEE Journal on*, vol. 28, no. 5, pp. 716–727, 2010.

[8] A. S. Malik, J. Kuang, J. Liu, M. Kamran, and Q. Liu, "Energy efficiency analysis of hybrid-mac protocols with application constraints in wireless sensor networks," in *Emerging Technologies, 2007. ICET 2007. International Conference on*, pp. 22–26, IEEE, 2007.

[9] L. Fang and R. J. de Figueiredo, "Energy-efficient scheduling optimization in wireless sensor networks with delay constraints," in *Communications, 2007. ICC'07. IEEE International Conference on*, pp. 3734–3739, IEEE, 2007.

[10] J. Li and P. Mohapatra, "Analytical modeling and mitigation techniques for the energy hole problem in sensor networks," *Pervasive and Mobile Computing*, vol. 3, no. 3, pp. 233 – 254, 2007.

[11] C. Ma, J. He, H.-H. Chen, and Z. Tang, "Coverage overlapping problems in applications of ieee 802.15.4 wireless sensor networks," in *Wireless Communications and Networking Conference (WCNC), 2013 IEEE*, pp. 4364–4369, April 2013.

[12] P. Sahoo and W.-C. Liao, "Hora: A distributed coverage hole repair algorithm for wireless sensor networks," *Mobile Computing, IEEE Transactions on*, vol. 14, pp. 1397–1410, July 2015.

[13] D. Pompili, T. Melodia, and I. F. Akyildiz, "Three-dimensional and two-dimensional deployment analysis for underwater acoustic sensor networks," *Ad Hoc Networks*, vol. 7, no. 4, pp. 778 – 790, 2009. I. Bio-Inspired Computing and Communication in Wireless Ad Hoc and Sensor NetworksII. Underwater Networks.

[14] K. Latif, M. Saqib, S. Bouk, and N. Javaid, "Energy hole minimization technique for energy efficient routing in under water sensor networks," in *Communication Technologies, Information Security and Sustainable Development* (F. K. Shaikh, B. S. Chowdhry, S. Zeadally, D. M. A. Hussain, A. A. Memon, and M. A. Uqaili, eds.), vol. 414 of *Communications in Computer and Information Science*, pp. 134–148, Springer International Publishing, 2014.

[15] H. Yan, Z. Shi, and J.-H. Cui, "Dbr: Depth-based routing for underwater sensor networks," in *NETWORKING 2008 Ad Hoc and Sensor Networks, Wireless Networks, Next Generation Internet* (A. Das, H. Pung, F. Lee, and L. Wong, eds.), vol. 4982 of *Lecture Notes in Computer Science*, pp. 72–86, Springer Berlin Heidelberg, 2008.

[16] A. Wahid and D. Kim, "An energy efficient localization-free routing protocol for underwater wireless sensor networks," *International journal of distributed sensor networks*, vol. 2012, 2012.

[17] M. Ayaz and A. Abdullah, "Hop-by-hop dynamic addressing based (h2-dab) routing protocol for underwater wireless sensor networks," in *Information and Multimedia Technology, 2009. ICIMT '09. International Conference on*, pp. 436–441, Dec 2009.

[18] E. Cayirci, H. Tezcan, Y. Dogan, and V. Coskun, "Wireless sensor networks for underwater survelliance systems," *Ad Hoc Networks*, vol. 4, no. 4, pp. 431 – 446, 2006.

[19] A. Sanchez, S. Blanc, P. Yuste, and J. Serrano, "A low cost and high efficient acoustic modem for underwater sensor networks," in *OCEANS, 2011 IEEE - Spain*, pp. 1–10, June 2011.

[20] A. F. Harris III and M. Zorzi, "Modeling the underwater acoustic channel in ns2," in *Proceedings of the 2nd international conference on Performance evaluation methodologies and tools*, p. 18, ICST (Institute for Computer Sciences, Social-Informatics and Telecommunications Engineering), 2007.

[21] M. Stojanovic, "On the relationship between capacity and distance in an underwater acoustic communication channel," *ACM SIGMOBILE Mobile Computing and Communications Review*, vol. 11, no. 4, pp. 34–43, 2007.

[22] J. U. Robert, "Principles of underwater sound," *New York: McGraw-Hill Book Company*, 1983.

[23] T. C. Austin, R. P. Stokey, and K. M. Sharp, "Paradigm: a buoy-based system for auv navigation and tracking," in *OCEANS 2000 MTS/IEEE Conference and Exhibition*, vol. 2, pp. 935–938, IEEE, 2000.

[24] C. Bechaz and H. Thomas, "Gib system: The underwater gps solution," in *Proceedings of 5th Europe Conference on Underwater Acoustics*, 2000.

[25] Y. Zhang and L. Cheng, "A distributed protocol for multi-hop underwater robot positioning," in *Robotics and Biomimetics, 2004. ROBIO 2004. IEEE International Conference on*, pp. 480–484, IEEE, 2004.

[26] K. M. Kwak and J. Kim, "Development of 3-dimensional sensor nodes using electro-magnetic waves for underwater localization," *Journal of Institute of Control, Robotics and Systems*, vol. 19, no. 2, pp. 107–112, 2013.

[27] K. Lorincz and M. Welsh, "Motetrack: A robust, decentralized approach to rf-based location tracking," in *Location- and Context-Awareness* (T. Strang and C. Linnhoff-Popien, eds.), vol. 3479 of *Lecture Notes in Computer Science*, pp. 63–82, Springer Berlin Heidelberg, 2005.

[28] A. Woo and D. E. Culler, *Evaluation of efficient link reliability estimators for low-power wireless networks*. Computer Science Division, University of California, 2003.

1530-437X (c) 2015 IEEE. Personal use is permitted, but republication/redistribution requires IEEE permission. See http://www.ieee.org/publications_standards/publications/rights/index.html for more information.